Condensation route of evolution of nanodispersed substances

I. V. Melikhov and V. E. Bozhevol´nov★

Department of Chemistry, M. V. Lomonosov Moscow State University,
1 Leninskie gory, 119992 Moscow, Russian Federation,
Fax: +7 (095) 932 8846. E-mail: melikhov@radio.chem.msu.ru

Numerous experimental data indicate that nanosystems develop by stages. The evolution route of closed nanosystems includes stages of nanoparticle nucleation, growth, ripening, and agglomeration, and texture and composition ordering. In closed systems, nanodispersed substances occur in the nano-state for a limited period of time, which can be changed by varying the supersaturation of the medium with respect to nanoparticles. Nanoparticles in open systems tend to degrade due to chemical transformations, dissolution, or evaporation and the lifetime of open systems can be estimated. At every stage of development of nanosystems, the rates of variation of the state parameters of nanoparticles fluctuate over a scale much exceeding the molecular scale. The behavior of the set of nanoparticles is described by a Fokker—Planck type equation, which may underlie the formulation of the principal equation of physicochemical evolution of nanosystem.

Key words: nanosystems, evolution, particle nucleation, growth of nanocrystals, agglomeration, composition and structure ordering, Fokker—Planck equation.

Introduction

Substances composed of nanometer-sized particles have always aroused the interest of researchers. In the last decade, this interest enhanced due to the prospects of nanotechnology.[1] A large body of data on the formation and subsequent variation of the properties of nanodispersed substances has been accumulated. Some of the regularities are considered in this study using the experimental results obtained mainly at the laboratory of Heterogeneous Processes, the Moscow State University.

In this paper, the behavior of nanosystems is considered in relation to the precipitation from aqueous solutions, condensation, and gas chemical reactions of model substances over rather narrow range of process conditions. However, this does not deprive the results of studies of the desired generality. All facts given below were interpreted resorting to mathematical models, which allow one to reveal the generality of the regularities found and to identify the range of conditions in which these regularities are significant. Comparison of the generalized mathematical models with experimental data demonstrates that all real sets of nanoparticles formed in homogeneous supersaturated media develop according to a unified scenario described below, which ends, most often, in their disappearance. Processes resulting in the degradation and disappearance of nanosystems can be appreciably retarded, which is the object of effort of synthetic chemists who attempt to stabilize nanoparticles to male them "nanoprocessable". In some cases, nanoparticles can be stabilized for fairly long periods of time. However, this does not violate the stages of the evolution route.

In this paper, we used a number of terms that require explanation because the terminology used to describe nanosystems has not yet been settled. A nanosystem is a set of nanoparticles occurring in the gas, liquid, or solid medium with a definite volume confined by walls. The term nanoparticles is accepted to mean particles with dimensions of 0.1—100 nm. Particles with dimensions of 0.1—100 μm are called microparticles, and larger ones are macroparticles. When the problems of mechanics are considered, they are referred to as nano-, micro-, and macrobodies, respectively. A set of nanoparticles that can be described by a definite chemical composition is called a nanodispersed substance, irrespective of whether it exists as a powder, a suspension, or an aerosol. When discussing the state distribution functions of nanoparticles, it is taken that fragmentation of macroparticles of a substance gives rise to the nanostate whose specific nature requires a special term.

Three routes to nanodispersed substances

A substance can be transferred into the nanodispersed state in three ways: by dispersing macroscopic bodies (fragmentation route), by evaporation or dissolution of macrobodies with subsequent formation of the nanobodies from the resulting vapor or solution (condensation route), and through a chemical reaction between macrobodies representing one reactant and a gas (or a liquid) as another

Published in Russian in *Izvestiya Akademii Nauk. Seriya Khimicheskaya,* No. 1, pp. 17—31, January, 2005.

1066-5285/05/5401-0016

reagent (topochemical route).[2,3] In the case of the fragmentation route, mechanical, electromagnetic, or thermal energy is pumped into the initial substance macrobodies in the pulse mode, thus exciting the macrobodies to such an extent that they decompose into nanofragments. In the condensation route, the vapor (or the solution) formed upon evaporation (dissolution) of macrobodies is made supersaturated and then bulk crystallization is triggered. In the topochemical route, sorption of the first reactant by the macrobodies of the second reactant is induced under conditions in which the reaction product separates in a nanodispersed state on the surface and in the bulk of the macrobodies.

The conditions for implementation of the three routes are diverse. However, in any case, each route includes the same pattern of alternation of elementary processes, resulting in a change in the properties of the nanodispersed substance. Therefore, the key features of the elementary processes that determine the evolution of the substance particles can be elucidated on the basis of one route, for example, the condensation one.

Condensation route of development of a closed system

It follows from experiment that if separate molecules of a given substance predominate in the system after supersaturation has been created, the formation of particles of this substance starts with the appearance of clusters composed of two or more molecules.[4] The clusters are formed *via* fluctuations. They appear and disappear, numerous formation and decomposition events resulting in the selection of the most stable configurations. The clusters are mainly enlarged upon the addition of single molecules, the addition being more frequent for higher supersaturation degrees; for invariable supersaturation, the addition frequency increases with an increase in the cluster size. The frequency of cluster decomposition depends only slightly on the supersaturation but decreases as the cluster becomes larger. As a consequence, small clusters are enlarged with a relatively low probability, but those that have been able to become larger start to grow rapidly.[5] A cluster that has occasionally reached the critical size at which the probability of its decomposition is equal to the probability of enlargement can be regarded as a nucleus of the substance particle. The formation of nuclei (nucleation) only from molecules of a given substance (homogeneous nucleation) is the fundamental process in the condensation route of evolution of a substance containing no admixtures.[6]

Supersaturated media always contain impurity nanoparticles, which are almost impossible to remove. The impurity nanoparticles adsorb molecules of this substance and can be converted into the particle nuclei if adsorption is polymolecular and occurs rather fast. When the supersaturation is relatively low, this transformation (heterogeneous nucleation) prevails over homogeneous nucleation. For high supersaturations, the homogeneous nucleation predominates. This was shown, in particular,[7] by direct determination of the nucleation rates in supersaturated aqueous solutions of ammonium chloride containing specified amounts of added nano- and microcrystals of strontium sulfate able to transform into the nuclei of NH_4Cl crystals.

The originated particles are enlarged due to the addition of separate molecules and small clusters and, later, due to the combination of particles with one another (Fig. 1). The rate G of enlargement upon the addition of molecules is given by

$$G = \upsilon_0[\omega(C/C_\infty)^n - \nu], \quad (1)$$

where υ_0 is the volume occupied by one molecule in the particle, ω is the probability of addition of a single molecule to the particle per unit time (calculated based on unit surface area of the particle), ν is the frequency of the removal of molecules from unit surface area of the particle to the medium, C is the concentration of the substance in the medium, C_∞ is its solubility, n is the sensitivity factor of the growth rate to the supersaturation.

The frequencies ω and ν depend on the particle size, shape, and composition. These properties are different for different particles; hence, each of them has its own rate G.[8]

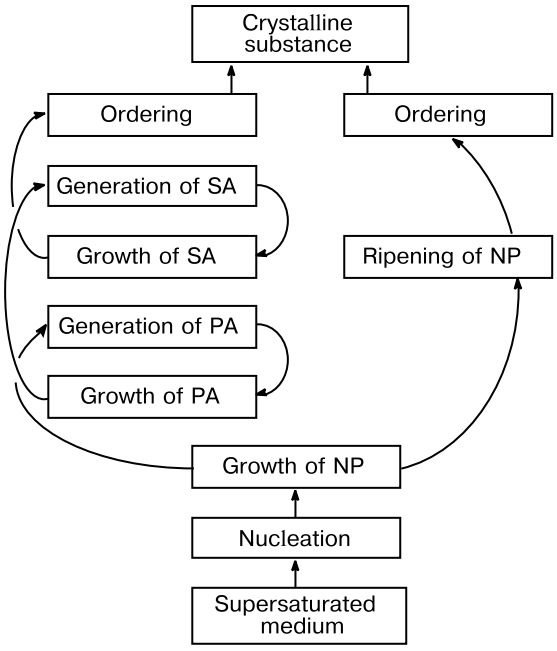

Fig. 1. Block diagram of the condensation route of the evolution of nanodispersed systems (NP are nanoparticles; PA are primary agglomerates; SA are secondary and larger agglomerates).

Direct measurements of the frequencies ω and ν for CaF_2 nanocrystals have shown[9] that the difference between these frequencies for various nanocrystals is mainly determined by differences between their sizes. The following relation is relevant

$$\nu = \omega\exp[(l_H n)/(l + l_0)], \quad (2)$$

where l is the effective particle size, l_H and l_0 are empirical coefficients characterizing the upper and the lower limits of the range of sizes in which a "strong" relationship between these frequencies exists.

Therefore,

$$G = \upsilon_0\omega\{(C/C_\infty) - \exp[(l_H n)/(l + l_0)]\}, \quad (3)$$

Due to the molecular growth of particles, the substance concentration in the medium decreases at the rate

$$-\frac{dC}{dt} = 4\pi\int_0^\infty G\rho l^2\varphi(l,t)dl, \quad (4)$$

where ρ is the number of moles of the substance per unit volume of the particle, $\varphi(l,t) = \partial N/\partial l$ is the size distribution function of the particles at time instant t, N is the number of particles with a size smaller than l in unit volume.

According to relations (3) and (4), at a particular instant t_R, the concentration C decreases down to

$$C = C_\infty\exp[l_H/(l_R + l_0)], \quad (5)$$

where l_R is the smallest size of particles that make a noticeable contribution to N.

At time t_R, particles with size l_R occur in the dynamic equilibrium with the medium, because the frequency of the addition of molecules to them is comparable with the departure frequency. Beginning from time t_R, the particle ripening begins. When $t > t_R$, the smallest particles start to dissolve (evaporate) and, after a while, they dissolve completely. Subsequently, due to the decrease in C, the dissolution starts to involve larger and larger particles. This goes on until the system contains only particles whose size is much greater than l_H.

The molecular growth of particles is usually complicated by aggregation. During aggregation, the particles that collide due to the Brownian motion or migration together with the medium stick together and are held in contact for a certain period. During this period, some of them coalesce to form agglomerates,[10] which serve as the nuclei for further agglomeration (Fig. 2). These nuclei grow upon successive adhering of new particles to them, similarly to the growth of a particle through addition of new molecules. After the formation of agglomerates, the particles incorporated in them remain individual for some period, but gradually the boundaries between them are "healed". However, if the mechanical energy is intensively supplied to the system, healing of the boundaries is counteracted by agglomerate loading, which can result in their fragmentation. All this has been revealed while observing natural processes and in experiments.[11,12]

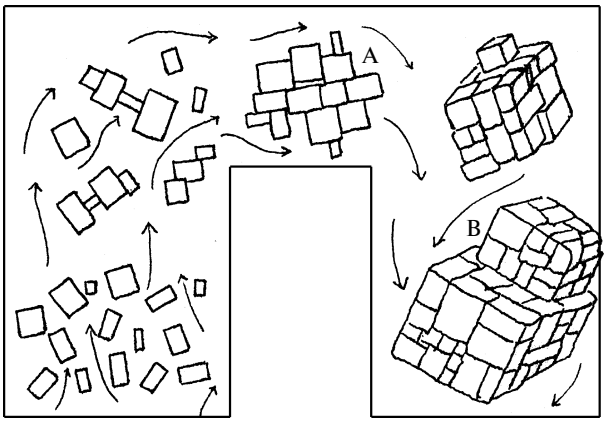

Fig. 2. Diagram of primary agglomeration in a suspension flow: A is a site favorable for the addition of a nanoparticle; B is the site for the addition of a primary aggregate.

The foregoing indicates that the condensation route of the development of a closed system includes the following stages: creation of supersaturation; particle nucleation, growth, and ripening described by relations (1)—(5); and agglomeration and agglomerate ordering, which may be counteracted by the supply of the mechanical energy to the system.

Nanostate life of a substance

According to experimental data, the properties of nanoparticles are so specific that one can speak of a specific nanostate of the material in which all properties of its particles $\{X_i\}$ depend sharply on their size and vary with time along an evolution route. Therefore, the complete characterization of a substance existing in the nanostate is provided by the property distribution function

$$\psi(X_i,t) = \frac{\partial^p E(t)}{\partial X_1 \ldots \partial X_p},$$

where $E(t)$ is the fraction of particles for which the state parameters that characterize the properties do not exceed simultaneously the $\{X_i\}$ values at time t, p is the number of properties involved in the consideration.

This function determines the set of application properties of a substance $\{\bar{X}_i\}$ such that

$$\bar{X}_i = \int_{-\infty}^{+\infty} X_i\psi(X_i,t)dX_1 \ldots dX_p.$$

However, the $\psi(X_i,t)$ function is difficult to derive. Therefore, for approximate characterization of the nanostate, one has to assume that all properties of a particle are

functionally related to its size; hence, instead of $\psi(X_i,t)$, one can use the $\varphi(l,t)$ function provided that

$$\bar{X}_i = \frac{1}{N_0}\int_{l_0}^{\infty} X_i\varphi(l,t)\mathrm{d}l, \qquad N_0 = \int_{l_0}^{\infty}\varphi(l,t)\mathrm{d}l,$$

where N_0 is the number of particles per unit volume of the system at instant t, l_0 is the minimum size for which the change in the state of the particle can be considered to be continuous.

Experimental data indicate that the function $\varphi(l,t)$ varies during the nucleation, growth, and ripening stages in conformity with the Fokker—Planck type equation

$$-\frac{\partial\varphi}{\partial l} = \frac{\partial}{\partial l}\left[G\varphi - \frac{\partial}{\partial l}(D\varphi)\right] \qquad (6)$$

for

$$\left[G\varphi - \frac{\partial}{\partial l}(D\varphi)\right]_{l\to l_0} = J,$$

$$\varphi(l,0) = 0, \qquad \varphi(\infty,t) = 0, \qquad (7)$$

where D is the fluctuation coefficient of the particle growth and J is the nucleation rate. The growth rate G is described by relations (1)—(3); for estimation, it can be assumed that

$$D = aG,$$

$$J = J_0\left[(C/C_\infty)^m - 1\right] + N_{\mathrm{Im}}\,\omega_{\mathrm{Im}}\exp\left(-\int_0^t \omega_{\mathrm{Im}}\mathrm{d}t\right), \qquad (8)$$

where a is the average fluctuation amplitude of the particle size, J_0 is the characteristic rate of homogeneous nucleation, N_{Im} is the number of impurity nanoparticles per unit volume of the initial system, ω_{Im} is the probability of transformation of the impurity nanoparticle into a nucleus per unit time, m is the sensitivity factor of the nucleation to the medium supersaturation.

Equations (6) and (7) describe the experimental data concerning the nucleation and growth of the CsI, NH_4Cl, NH_4Br, and $ZrCl_4$ nanocrystals in the vapor phase, the formation of amorphous Al_2O_3 nanoparticles upon hydrolysis of the $AlCl_3$ vapor, the formation of the $Fe(OH)_3$ nanoparticles upon alkalification of $FeCl_3$ solutions, and in many other cases.[13—17] Therefore, relations (6) and (7) underlie the formulation of the principal evolution equation for the variation of the state distribution function of particles with time. The formulation implies the identification of the development of the G, D, and J values for the state parameters $\{X_i\}$ of particles and the properties $\{y_i\}$ of the medium.

The general form of the functions

$$G = G(X_i,y_i),$$

$$D = D(X_i,y_i),$$

$$J = J(y_i)$$

has not been elucidated as yet. However, a large number of data attest to abundance of systems to which relations (3) and (8) are applicable.

Equations (3)—(8) determine a number of conditions under which the substance can occur in the nanostate.

The solution of Eqs. (6)—(8) showed that in a closed system where

$$a = \mathrm{const}, \qquad J_0 \gg N_{\mathrm{Im}}\omega_{\mathrm{Im}},$$

$$C_0 \gg C_\infty\exp[l_{\mathrm{H}}/(l_{\mathrm{R}} + l_0)]$$

the nucleation and the growth are almost completed over a period of time comparable with the value

$$t_1 = 2A_1\Big/\left(\upsilon_0\omega\sqrt{0.1 + a/A_1}\right) \qquad (9)$$

for

$$A_1 = \left[\frac{\upsilon_0\omega C_\infty}{(4\pi/3)\rho J_0}\left(\frac{C_0}{C_\infty}\right)^{1-q}\right]^{1/4},$$

where C_0 is the substance concentration in the initial medium, $q = m - n$.

The average particle size at time instant t_1 and at usual values of $q < 10$ reaches

$$\bar{l} = (0.74 + 0.14q)A_1$$

for the variation coefficient

$$K = 0.52(q + 0.75)^{-0.35} + 0.74(a/A_1)^{0.86}(q + 1)^{0.35} \qquad (10)$$

and the size dispersion $\sigma^2 = (K\bar{l})^2$. The maximum particle size $l_{\max}$ (the size greater than the sizes of 95% of the particles) is close to the value

$$l_{\max} = \bar{l}\,(1 + 1.5K).$$

It follows from these relations that under conditions (6) and (7), a substance occurs in the nanostate at time t_1 provided that

$$\left(\frac{C_0}{C_\infty}\right)^{(q-1)/4} \geq (0.74 + 0.14q)(1 + 1.5K)(L_2/L), \qquad (11)$$

$$L_2 = \left(\frac{3\upsilon_0\omega C_\infty}{4\pi\rho J_0}\right)^{1/4},$$

where L is the upper limit of the nanorange, L_2 is the characteristic particle size of the given substance.

Condition (11) reflects the fact that in the condensation route, a nanodispersed substance is formed only at $q > 1$ and a high supersaturation of the medium.

In a closed system under condition (11), a substance exists for some period in the nanostate from where it is led out by ripening. As has already been noted, the ripening starts at instant t_{R} when the concentration of the medium

decreases down to a level defined by relation (5). Experiments show that for estimates, it can be taken that $t_1 = t_R$ at $l_R = \bar{l}\,(1 - 2K)$.

When $t > t_1$, the dissolving smaller particles maintain supersaturation of the medium, thus facilitating the growth of larger particles. The rate of the particle growth at $l > l_B$ is given by

$$G = \upsilon_0\omega\left[\exp\left(\frac{nl_H}{l_0 + l_B}\right) - \exp\left(\frac{nl_H}{l_0 + l}\right)\right], \qquad (12)$$

where l_B is the boundary size that separates the fractions of dissolving and growing particles at the instant when the frequency of addition of molecules to the growing particles is equal to ω. The boundary size

$$l_B = l_H/\ln(C/C_\infty) - l_0.$$

When $t \to t_2$, the largest particles reach the upper boundary L of the range of nano-sizes. From this moment, the substance starts to depart from the nanostate. The departure is over at instant t_3, when almost all growing particles have reached the boundary L. The time span from the instant the supersaturation is created up to instant t_3 is the period the substance exists in the nanostate. The time span from t_2 to t_3 is the period of nanostate elimination.

The time the substance exists in the nanostate can be varied by varying the supersaturation at the ripening stage. Indeed, if the substance concentration in the medium is maintained at $C = C_R$ from time t_R, then the t_2 and t_3 periods would be shortened as much as possible. In this case, all particles except for the smallest ones would grow, the boundary value $l_B = l_R$ remaining invariable. The growth rate $G = \mathrm{d}l/\mathrm{d}t$ would increase with time according to Eq. (12). The approximate integral of this equation for $nl_H \ll l_B$ has the form

$$t - t_1 = B_1F(l,l_1), \qquad (13)$$

$$F(l,l_1) = \frac{l - l_1}{l_0 + l_R} + \ln\left(\frac{l - l_R}{l_1 - l_R}\right),$$

where $B_1 = (l_0 + l_R)^2/(\upsilon_0\omega nl_H)$, l and l_1 are the sizes of the given particles at times t and t_1.

It follows from relation (13) that

$$t_2 = t_1 + B_1F(L,l_{max}), \qquad t_3 = t_1 + B_1F(L,l_s), \qquad (14)$$

where $l_s = \bar{l}\,(1 - K)$.

The t_2 and t_3 values are not strictly definite, as they reflect the uncertainty in selecting the l_{max} and l_s. However, more precise estimates will not change the general picture.

Relations (12)—(14) define the conditions that allow one to shorten the times t_2 and t_3 by increasing the substance concentration in the medium during ripening. Analogous relations are suitable to estimate the conditions under which the residence time of the substance in the nanostate can be increased.

Stages of development of the nanosystem

In a closed system, a nanodispersed substance is formed by stages (see Fig. 1). At the first stage, when nucleation and nanoparticle growth predominate in the system, the rate of substance accumulation in nanoparticles increases. Subsequently, this rate decreases to a level where ripening of the new phase starts. During the second stage when the ripening and agglomeration predominate, this rate continues to decrease but much more slowly than at the end of the first stage. If agglomeration proceeds faster than ripening, the second stage is followed by the third stage in which ordering of the internal structure of the agglomerates is the predominant process. The duration of the first stage is determined by relation (9), and that of the second stage, by relation (14). The ordering of agglomerates requires time commensurable with the value

$$t_4 = X_1^2/q_s, \qquad (15)$$

where X_1 is the agglomerate size, q_s is the diffusion coefficient of atoms in the particle bulk.

Observations showed that in all of the systems we studied, agglomeration is much slower than the nanoparticle growth. The nanoparticles are quickly joined into disordered aggregates (floccules), but their ordering proceeds slowly.

Examination of the floccules of $Fe(OH)_3$ and $Ca_3(PO)_2$ formed in an aqueous medium at 300 K has shown that both have irregular shape, which in some cases approaches a spherical shape. The floccules are not fractals. Their size and shape change markedly even on minor variations of the intensity of movement of the medium. The nanoparticles inside the floccules form a network structure in which the fraction of the nanoparticle surface area that falls on their contacts with one another is not greater than several percent. In the floccules of the $Fe(OH)_3$ nanoparticles having a filamentary shape, the nanoparticles contact mainly by the ends of the threads. In the floccules composed of the lamellar calcium phosphate nanoparticles, some of them contact by the bases of the plates, and other, by the lateral faces of the plates, giving rise to a network structure. In both cases, the formation of floccules is the first stage in the spatial ordering of the nanosystem. Similar floccules were detected in a sharply cooled CsI vapor.

Subsequently, groups of accreted nanoparticles, which are the nuclei of agglomerates, are formed either inside or outside the floccules. These nuclei are mainly enlarged through the addition of separate nanoparticles, similarly

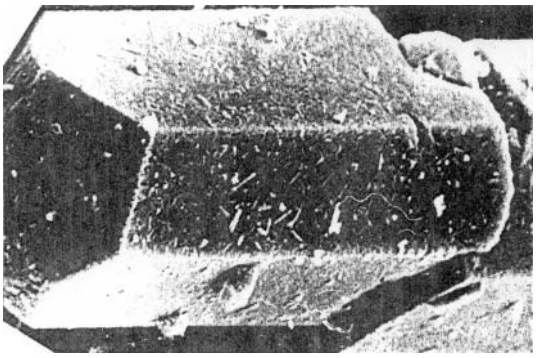

Fig. 3. Polyhedral secondary agglomerate of $CaSO_4 \cdot 0.5H_2O$ nanocrystals formed in a moving suspension ($T = 353$ K, phosphoric acid medium, supersaturation $\xi = 1$, Reynolds number Re = 170, enlargement time $t = 1.6 \cdot 10^4$ s).

to the growth of nanoparticles through the addition of molecules. If the nanoparticles are polyhedral, the agglomerates also tend to acquire a polyhedral shape (Fig. 3). The nanoparticle growth and agglomeration steps prove to be kinetically similar: in both stages, the change in the state of particles can be described by the same equation where the states of the primary nanoparticles and agglomerates are characterized by the same state parameters $\{X_i\}$ (Fig. 4). The kinetic similarity of the stages seems to be an important feature of the development of these nanosystems.[13,14]

If a sufficient amount of mechanical energy is supplied to the system, agglomeration becomes multistage. If the suspension is stirred rather vigorously at the end of the agglomeration stage, the disordered agglomerates of an irregular shape are destroyed. Densely packed agglomerates are accumulated in the system and gradually they acquire a polyhedral shape. As time elapses, most of nanoparticles find places in the agglomerates where they are held rather firmly in order to resist the destruction (see Fig. 2). Gradually, the agglomeration slows down, which can be considered as completion of its first stage. A regular shape of the agglomerates formed at this stage (primary agglomerates) is not favorable for their joining into secondary agglomerates. Nevertheless, groups of accreted primary agglomerates whose shape is favorable for enlargement are accumulated in the suspension. The appearance of these groups (which are the nuclei of secondary agglomerates) results in acceleration of the agglomeration, *i.e.*, in the beginning of the second agglomeration stage in the system. The pattern of multistage agglomeration discovered in a suspension of $BaSO_4$ nanocrystals in a supersaturated aqueous solution is shown in 5. The multistage pattern of the agglomeration is manifested in the fact that the agglomerates acquire an hierarchical structure, which becomes more complicated from one stage to another.

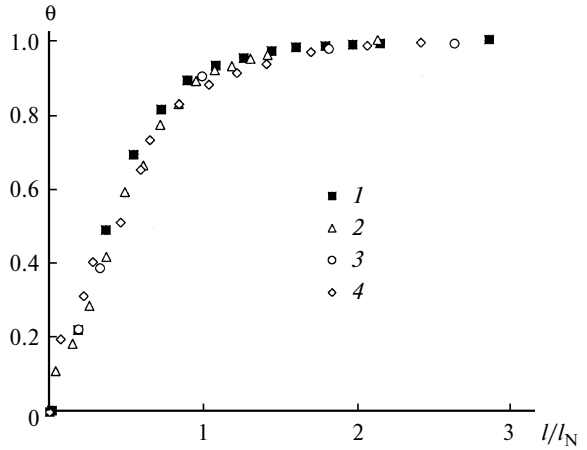

Fig. 4. Integral distribution functions of nanocrystals and primary and secondary agglomerates of hydroxyapatite (sample was prepared by the jet method at 300 K; θ is the fraction of particles whose size is smaller than l; l_N is the normalizing factor): (*1*) primary nanoparticles (l_N = 20 nm), (*2*) primary agglomerates (l_N = 500 nm), (*3*) secondary agglomerates (l_N = 7 μm), (*4*) secondary agglomerates after boiling (l_N = 150 μm).

Nanosystem variability

The variability of nanosystems implies that the rates of processes in their bulk are highly sensitive to minor changes in conditions. There exist mechanisms in nanosystems that enhance minor fluctuations and bring them to a macroscopic scale.[18,19] Due to these mechanisms, under almost identical conditions when fluctuations in

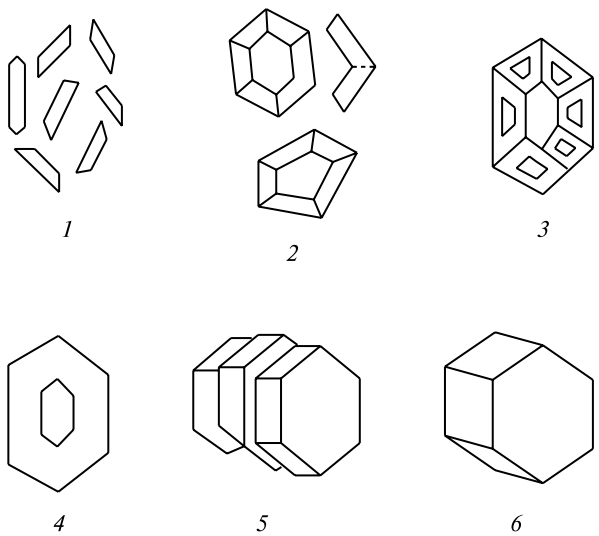

Fig. 5. Change in the particle shape of barium sulfate during their formation in an aqueous solution with a high initial supersaturation: (*1*) filamentous nanocrystals, (*2*) primary ring agglomerates, (*3*) and (*4*) secondary ring agglomerates before and after morphological ordering, (*5*) and (*6*) tertiary agglomerates before and after the morphological ordering.

the operation of devices that control the processes do not exceed the mechanical tolerance, processes may occur at essentially different rates and result in essentially different property distribution functions of the substance particles.

The nucleation process is especially variable. One factor responsible for the variability of nucleation is supersaturation. In the case of low supersaturations, the nucleation rate is relatively low. The increase in the supersaturation up to a certain "critical" level (metastability boundary) results in a sharp acceleration of nucleation.[20] In some systems, this acceleration is so pronounced that uncontrolled overstepping of the metastability boundary may induce unexpected nucleation surges.

In the media with low supersaturation in which heterogeneous nucleation predominates, uncontrolled admixtures that change the particle nucleation and growth rates are mainly responsible for the variability. Thousands of substances able to pass into liquid or gas media have been detected in the atmosphere. Many of these substances occur in the air as nanoparticles whose concentration is 10^{11}—10^{14} m^{-3} under ambient conditions and cannot be reduced below 10^8 m^{-3} even by a thorough purification.[21] Therefore, any environment contains hundreds admixture substances as molecules and nanoparticles, the amount of each admixture depending on the medium prehistory, which is unique. The results of continuous monitoring of the radioactivity of the air as it passes through a measuring chamber mounted in a region of Serbia provide as example of oscillations of the admixture content in the environment (Fig. 6). This radioactivity was due to the decay of ^{212}Pb that entered the detector together with the air, so that the oscillations of the radioactivity level reflected the fluctuations of the admixture concentrations in air.[22]

Real environments most often contain admixture microcrystals, which are also difficult to remove. The surface of the admixture microcrystals usually has active sites on which the nuclei of the substance are formed. This was demonstrated in relation to a celestine ($SrSO_4$) crystal placed in a supersaturated aqueous solution of K_2SO_4.[23] It was found that a fairly large number of K_2SO_4 microcrystals nucleate and grow on the crystal surface at

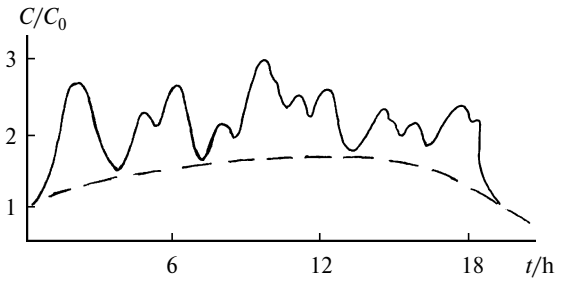

Fig. 6. Results of the continuous monitoring of the radioactivity of the near-surface air in a Serbian region[22] (C and C_0 are the current and initial concentrations of ^{212}Pb in air).

the supersaturation $\xi_0 = 0.6$ and a temperature of 288 K. During the second exposure of this crystal in a solution with the same properties, the time that elapsed before microcrystals appeared on each surface microsection was different. On the same microsection and seemingly under the same conditions, a microcrystal appeared sometimes within minutes and sometimes within hours. Generally, the microcrystals were distributed over the nucleation frequencies according to the broad Raley distribution.

The admixture microcrystals can be represented by nano- and microcrystals of the same substance formed earlier. Under certain conditions, these seed crystals can induce the secondary nucleation, one crystal being able to give rise to a multitude of particles of this compound (nucleation avalanche). In the case of formation of this avalanche, the occasional formation of single seed crystals in the initial medium can induce transition of the whole system into the nanostate. Transition of this type has also been detected on decomposition of solid solutions, CaF_2—GdF_3, CaF_2—EuF_3, and CaF_2—TbF_3.[24—26]

It was found that a single crystal of a solid solution grown by the Bridgman method (by drawing the crystal from a CaF_2 melt containing EuF_3) and cooled can be converted into a supersaturated medium in which EuF_3 particles may nucleate. The nucleation probability is relatively low; therefore, the first nuclei appear rather rarely in the single crystal bulk. When the EuF_3 concentration is 5 mol % and the temperature is 900 K, the frequency of the appearance of primary seeds amounts to $\sim 5 \cdot 10^{10}$ m^{-3} s^{-1}. Each primary seed triggers the appearance of the EuF_3 nanoparticle bunches (Fig. 7). The nanoparticles are not manifested in the X-ray diffraction patterns of the single crystal and do not deteriorate its optical properties. Their number increases with time and they coherently grow together, thus forming the microcrystals of europium trifluoride. Thus, the transition of europium trifluoride from the solid solution into the nanostate is accelerated by the secondary nucleation, which gives rise to nanoparticle bundles, apparently, due to the development of nucleation avalanches.

In liquid media with low supersaturation, the reproduction of particles through the secondary nucleation takes place with intense supply of mechanical energy to the system. The reproduction intensity depends on the way of mechanical energy supply and the design features of the reactor; minor modifications in the reactor shape may give rise to pronounced effects. For example, in the polythermal crystallization of ammonium perchlorate NH_4ClO_4 from an aqueous solution in a crystallization beaker with a stirrer, the size of the production particles proved to be sensitive to the width of the gap between the stirrer and the beaker bottom. In repeated experiments, the gap width was maintained equal within the mechanical tolerance. However, this did not ensure an equal number of particles in the crystallization vessel at the end of

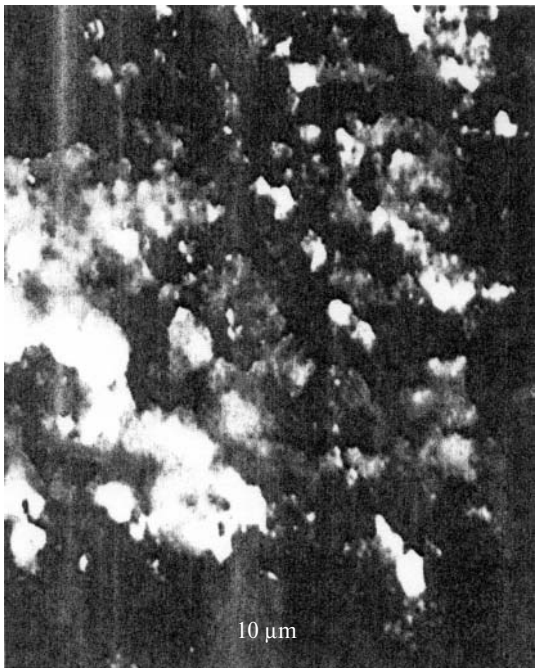

Fig. 7. Bunches of EuF_3 nanoparticles in the bulk of the CaF_2 single crystal prepared from a melt by the Bridgman method.

each experiment. The results of repeated experiments showed a distribution over the number of production particles (N_F) in the vessel according to a broad distribution function (Fig. 8). The difference between the number of production particles was due to fluctuations of the gap width, which proved to be significant, although remained within the limits of the mechanical tolerance. This conclusion is confirmed by the fact that a sharp increase in the gap width resulted in an equally sharp displacement of the distribution function $\varphi(N_F)$ toward smaller N_F. Apparently, narrowing down of the gap promoted the reproduction of microcrystals, while the reproduction changed this function.

In the media with high supersaturations, the fluctuations of the nucleation rate are mainly due to the system inhomogeneity. In order to create higher supersaturations, substances and energy should be supplied to the system with high intensity, which is associated with an increase in the gradients of the properties of the medium and flow turbulization. This gives rise to a random distribution of the medium supersaturation over the system bulk and oscillations of the nucleation frequency.

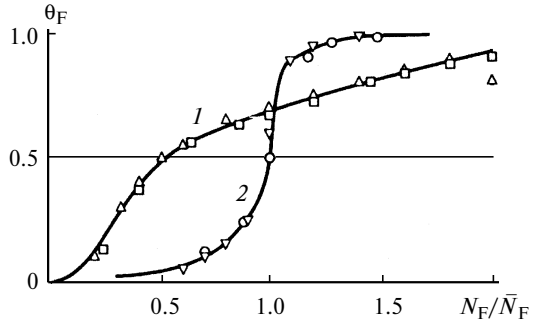

Fig. 8. Distribution of successive crystallizations of ammonium perchlorate over the numbers of particles formed in the crystallization tank by the end of the process. The gap between the edge of the stirrer and the tank bottom is 2.28±0.06 mm (*1*) or 11.64±0.09 mm (*2*); θ_F the fraction of crystallizations in which the particle number is smaller than N_F, $\bar{N}_F$ is the average value for a series of crystallizations.

Role of growth rate fluctuations

According to experimental data, the crystals occurring simultaneously in the same solution grow at different rates, the instantaneous growth rate of each crystal fluctuating with time, *i.e.*,

$$G_M \equiv dl/dt = G + \xi(l,t),$$

where G is the rate of directional change in the crystal size, $\xi(l,t)$ is a random function that describes the amplitude of the deviations of the instantaneous growth rate from G.

The rate G may be substantially different for crystals with different defectiveness, and the function $\xi(l,t)$ can apparently have different forms. The results of measurements of the growth rate for one face of a single microcrystal of the $CaSO_4 \cdot 2H_2O$ dihydrate in a steady-state flow of a supersaturated solution are shown in Fig. 9. This rate is the result of averaging of the instantaneous rate over a short interval Δt and, therefore, it is close to G_m. The amplitude of fluctuations of the rate G_m is commensurable with the rate G, *i.e.*, this is a macroscopic value. The $\xi(l,t)$ function was found to be centered and delta-correlated.

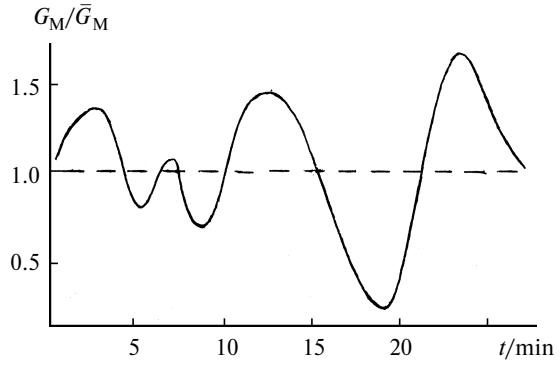

Fig. 9. Growth rate of the (001) face of the calcium sulfate dihydrate microcrystal growing in a steady-state flow of a supersaturated aqueous solution; $\bar{G}_M$ is the average rate for a 3 h observation.

Table 1. Experimental data on the scale of fluctuations of the particle growth rate in an aqueous medium at 295 K

Compound	$\bar{l}$ /nm	a/nm	$a/\bar{l}$
$BaSO_4$	1.53±0.02	0.5	0.3
$Fe(OH)_3$	1.75±0.09	0.035	0.02
CaF_2	4.0±0.3	0.08	0.02
$BaCO_3$	4.16±0.04	1.0	0.25
$BaSO_4$	8.0±0.1	1.0	0.12
$Ca_3(PO_4)_2$	29.2±0.03	2.2	0.07
$Cd(OH)_2$	30±1	1.0	0.03
$Mg(OH)_2$	30±1	0.5	0.015
$ZnC_2O_4 \cdot 2H_2O$	150±5	1.3	0.01
$BaSO_4$	$(5.0\pm0.01)\cdot10^3$	250	0.05
NaCl	$(1.0\pm0.01)\cdot10^4$	400	0.04

The magnitude of the growth fluctuations of the nanocrystals can be estimated from published data,[27] which states that the rate of propagation of the monolayer over the surface of the growing $BaSO_4$ nanocrystal can randomly change several-fold. Substantial fluctuations of the growth rate are also indicated by high magnitudes of parameter a given in Table 1.

The parameter a was determined by comparing the experimental data on the function $\varphi(l,t)$ with the results of numerical solution of Eqs. (6)—(8) and minimizing the deviations of the calculated data from experimental ones. In all these systems, the change in the distribution function upon variation of the parameter a is not sufficiently pronounced to enable accurate determination of its values. However, the estimates presented in the Table 1 seem reliable. The a value characterizes the deviation of the growth front from ordered motion caused by fluctuations. It can be seen that the scale of such deviations is much greater than the molecular scale.

The main reason for the macroscopic fluctuations of the growth rate is the cooperative interaction of atoms, manifested as the formation of two-dimensional clusters on the surface of growing particles. The relationship between the fluctuations and two-dimensional clusters has been repeatedly identified experimentally. For example, it was found that the atomically smooth face of an Ag single crystal placed in a slightly supersaturated solution does not grow until a cluster of closely spaced adsorbed Ag atoms (two-dimensional nucleus) is formed on its surface. The two-dimensional nucleus rapidly spreads over the face, which becomes covered by a monolayer of atoms. After that, the face does not grow again until the next two-dimensional nucleus is formed on the surface, and so on. During the waiting periods for the two-dimensional nuclei, the instantaneous rate of the single crystal growth is equal to zero, while that during the monolayer deposition sharply increases.[28] This is due to the fact that for an Ag atom that passes to the surface from a solution, it is much more difficult to become attached to the atomically smooth face than to stick to the atomic group of a two-dimensional nucleus. Whereas the formation of the two-dimensional nucleus is a molecular-scale fluctuation, the deposition of the monolayer represents the development of the molecular fluctuation to a macroscopic scale. This development takes place in all systems in which the parameter a satisfies the condition

$$a \gg \upsilon_0/4\pi l^2. \qquad (16)$$

When condition (16) is fulfilled, then in closed systems at the nucleation and growth stages, Eq. (6) is applicable and nanoparticles have a broad size distribution. If $G \neq G(l)$, the size dispersion increases by a square law according to relation (10) as the nanoparticles are enlarged. The increase in the dispersion continues at the beginning of the ripening stage. The dispersion decreases only by the end of ripening. However, long before this decrease, almost all nanoparticles exceed the bounds of the nanorange of sizes. Within the nanorange, the dispersion increases monotonically with particle enlargement if the growth rate does not depend on the size. If the growth rate decreases with enlargement of nanoparticles, the dispersion may decrease with time, which is usually utilized in attempts to prepare monodisperse substances.[29]

Fluctuations of the growth rate are favorable for faster segregation of the nanodispersed substance from the supersaturated medium. This can be derived from relation (9), which implies that an increase in a entails a decrease in the time t_1 needed for the segregation of the main bulk of the substance. However, the variation coefficient of the nanoparticle size simultaneously increases (Eq. (10)), *i.e.*, the degree of ordering of the substance in the space of sizes. Thus, the fluctuations of the growth rate result in a faster formation of the nanodispersed material, which is, however, less ordered.

Apparently, a similar situation occurs in the agglomeration phase in which the agglomerates have already grown to a size much exceeding the nanoparticle size but still capture more nanoparticles. This is indicated by the kinetic self-similarity of the growth and agglomeration stages.

Spontaneous ordering of the particle structure

The inner state parameters of the nanoparticles and agglomerates continuously change. Particles get free from excess admixturies they have captured in the fast growth stage. If the particles are initially amorphous, they are transformed into nanocrystals. If the particles are formed as nanocrystals, the structural growth defects are "healed" in their bulk and their habitus approaches the equilibrium one. All these processes are versions of the internal order-

ing of particles, *i.e.*, they promote the particle properties toward those of a perfect crystal. The disorder of a separate particle can be expressed by the coefficient

$$Z(X_i,t) = \sum_{i=1}^{p}\left[\frac{1}{p}\left(\frac{X_i}{X_{iE}} - 1\right)^2\right],$$

where X_{iE} is a state parameter of a reference crystal.

In the case of crystalline substances,

$$\{X_i\} = \bar{b}, W_{di}, W_{Ii}, q_i,$$

where $\bar{b}$ is the average "interatomic" distance, W_{di} and W_{Ii} are the numbers of structural defects and admixture atoms of one sort in the crystal bulk, q_i is the fraction of atoms emerging onto one crystal face.

The disorder of all particles in the system is described by the coefficient

$$Z(t) = \frac{1}{N_0}\int_0^{\infty} Z(X_i,t)\varphi(X_i,t)\mathrm{d}X_i.$$

Under condition (11), which ensures the formation of substance in the nanostate, amorphous particles are often formed and subsequently they are transformed into crystals. The transformation takes place either through dissolution of amorphous particles with simultaneous crystal nucleation and growth (recrystallization route) or by transformation of every amorphous particle into a crystal without dissolution (topochemical route). The transformation by a recrystallization route has been detected in the precipitation of potassium polyvanadate from an aqueous medium. The topochemical route is involved in the transformation of amorphous tricalcium phosphate into hydroxyapatite. In this case, as shown by high-resolution electron microscopy (Fig. 10), numerous crystalline nanosections are formed rather slowly in the bulk of each primary amorphous nanoparticle; the combination and coherent accretion of these nanosections gives rise to hydroxyapatite nanocrystals.[30] The interatomic distances in the hydroxyapatite nanocrystals virtually do not differ from the distances in the reference single crystals. No dislocations were detected in the nanocrystal bulk, *i.e.*, the nanocrystals are distinguished by low structural disorder. However, they are essentially morphologically disordered, their shape changing with time from ~1 nm thick plates to isometric hexagonal prisms typical of bulk hydroxyapatite crystals.

The low structural disorder of the hydroxyapatite nanocrystals is, apparently, a consequence of their relatively slow formation. If nanocrystals are formed rapidly, their disorder is usually high.

One reason for the structural disorder of nanocrystals is the formation of growth vacancies. During the crystal growth, some of the point positions of the crystal lattice remain vacant. As a result, the density of the growing crystals is lower than the density of crystals that do not grow and the self-diffusion in their bulk is more intensive than that at thermal equilibrium. In particular, the density of the $CaSO_4 \cdot 2H_2O$ microcrystals after completion of the growth is 4—5% lower than that of the perfect crystals, this decrease being due to the growth vacancies, as demonstrated by positron defectoscopy.[31] The self-diffusion coefficients of the growing $BaSO_4$ microcrystals are 4—8 orders of magnitude greater than those of the equilibrium crystals.[32,33]

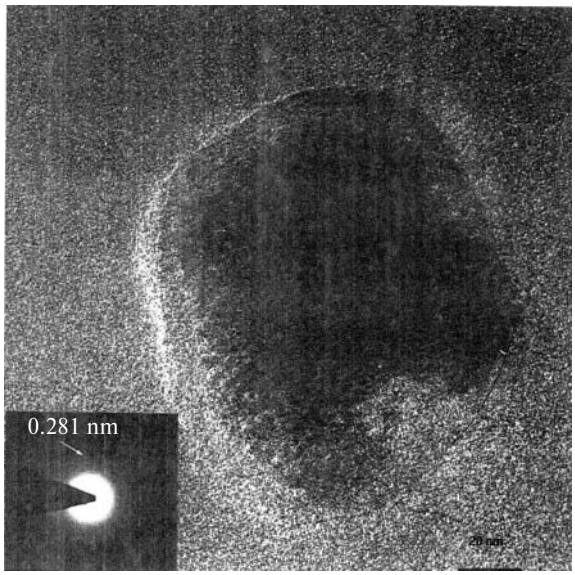

Fig. 10. Electron micrographs of a calcium phosphate particle at early stage of isolation from a supersaturated aqueous solution. In the amorphous body of the particle, one can see the crystal nuclei with sizes comparable with the size of the hydroxyapatite unit cell.

The simplest interpretation of these facts as applied to nanocrystals that grow by the layer-by-layer mechanism in a supersaturated solution is as follows. During the layer-by-layer growth, two-dimensional clusters rarely originate but rapidly spread over the crystal surface (Fig. 11). During the spreading, each cluster captures an excess amount of the solvent, while a large number of points in its lattice remain vacant. This is followed by cluster ordering, and its properties approach those of the surface monolayer of a perfect nanocrystal. The ordering is relatively fast until the crystal surface is coated by the next cluster. When this takes place, the molecules of the given cluster lose mobility and the ordering is sharply retarded. As a result, the solvent and the vacancies that occurred in the cluster at the coating instant pass to the crystal bulk.

During the period of time τ between the coverings of some section of the surface by this and next clusters, the

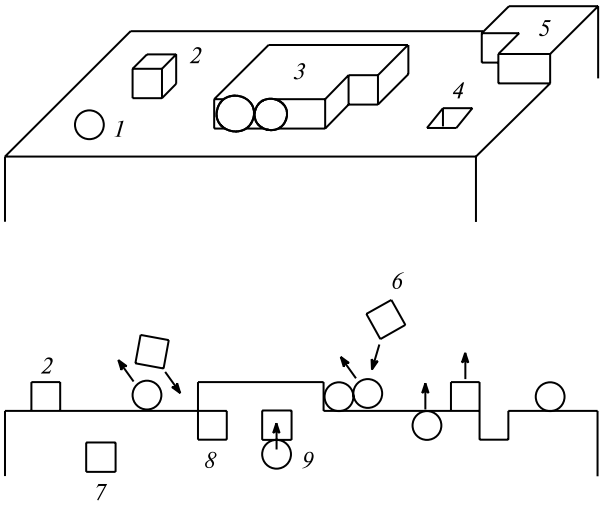

Fig. 11. Surface structures formed during the nanocrystal growth: (*1*) adsorbed solvent molecule, (*2*) adsorbed molecule of the major substance, (*3*) two-dimensional cluster on the face, (*4*) vacancy in the surface monolayer, (*5*) two-dimensional cluster at the crystal vertex, (*6*) molecule coming from the medium, (*7*) immured vacancy, (*8*) vacancy covered by the cluster, (*9*) internal solvent molecule.

proportion W of the vacant point positions in the section varies at the rate

$$dW/dt = \nu_{SL}W_L + \nu_{SM}(1 - W_L - W) - \nu W$$

for $t = 0$—$\tau = h/G$,

where ν_{SL} and ν_{SM} are the probabilities that solvent molecules and molecules of the major component will be removed from the surface monolayer to the solution per unit time; W_L is the fraction of the point positions occupied by the solvent; ν is the probability of filling a vacancy per unit time; and h is the monolayer thickness.

It can be written that

$$W(0) = W_0, \qquad W_L(0) = W_{L0},$$

$$\nu = \omega_L C_L + \omega_M C_M + \nu_V,$$

$$dW_L/dt = \omega_L C_L W - \nu_{SL}W_L,$$

where W_0 and W_{L0} are the fractions of vacant points and those occupied by the solvent immediately after the section has been covered by the cluster, ω_L and ω_M are the frequencies of transition of the solvent and matrix substance molecules from unit bulk of solution to the monolayer vacancies, C_L and C_M are the concentrations of the solvent and the matrix substance in solution, ν_V is the probability that the vacancy will pass to the nanocrystal bulk per unit time.

At time τ, the W and W_L values are equal to $W(\tau)$ and $W_L(\tau)$, which gives the concentrations of vacancies and solvent molecules that have passed to the crystal bulk

$$W_T = \chi_W(G)W(\tau), \qquad W_{LT} = \chi_L(G)W_L(\tau),$$

where $\chi_W(G)$ and $\chi_L(G)$ are functions that describe the behavior of vacancies and the solvent as this section is being coated by the next cluster.

It follows from the foregoing that if the condition

$$\nu_{SL} \gg \omega_L C_L, \nu_{SM},$$

holds, so that the crystal contains virtually no solvent molecules at equilibrium, then

$$W_T = \chi_W(G)\{W_E + (W_0 + \Phi - W_E)\times \times\exp[-(\nu + \nu_{SM})h/G] - \Phi\exp(-\nu_{SL}ah/G)\}, \qquad (17)$$

where $W_E = \nu_{SM}/(\nu + \nu_{SM})$ is the equilibrium concentration of vacancies in the monolayer,

$$\Phi = W_{L0}(\nu_{SL} - \nu_{SM})/(\nu_{SL} - \nu_{SM} - \nu).$$

According to relation (17), at high supersaturations, when the condition

$$G \sim h/\nu_{SL} \gg h/(\nu + \nu_{SM}),$$

$$G \sim h\nu_{SL} \gg h(\nu + \nu_{SM}), \qquad (18)$$

is fulfilled, the concentration of vacancies in the crystal grows as G decreases. Under these conditions, when $\chi_W(G) = \chi_W$,

$$W_T = \chi_W\{W_0 + \Phi[1 - \exp(-\nu_{SL}h/G)]\}.$$

When condition (18) is fulfilled, the change in the number of vacancies in the crystal is determined by the departure of solvent molecules from the monolayer, the possibility of such departure increasing with a decrease in G.

When the growth rate has decreased down to a level such that

$$G \sim h(\nu + \nu_{SM}),$$

the concentration W_T starts to decrease following the decrease in G to approach the equilibrium value. In addition,

$$W_T = \chi_W\{W_E + (W_0 + \Phi - W_E)\exp[-(\nu + \nu_{SM})h/G]\},$$

so that the disorder coefficient is

$$Z(W,t) = (W_0 + \Phi - W_E)\exp[-(\nu + \nu_{SM})h/G].$$

It can be seen that within the framework of this model, the disorder of the growing crystal varies non-monotonically following a decrease in the growth rate. At high rates, the concentration of vacancies increases with a decrease in G due to vacation of the point positions occu-

pied by solvent molecules. At low rates, the vacancy concentration diminishes with a decrease in G as the excess vacancies are filled by molecules of the matrix substance. Correspondingly, the vacancy disorder factor first increases and then decreases. However, this does not mean that the full disorder coefficient $Z(X_i,t)$ also varies nonmonotonically as the growth is retarded. The increase in $Z(W,t)$ at high G is accompanied by a decrease in the disorder coefficient of the crystal composition, related to the release of the solvent captured out of equilibrium.

Ordering of the particle composition

During fast growth, the nanocrystals capture excess amounts of those admixtures for which the equilibrium co-crystallization coefficient is smaller than unity and deficient amounts of admixtures for which this coefficient is greater than unity. In particular, the $BaSO_4$ nanocrystals and their agglomerates that are formed in aqueous media on mixing solutions of K_2SO_4 and $BaCl_2$ capture substantial excessive amounts of water, KCl, and K_2SO_4. These admixtures having a low co-crystallization coefficient are released to the medium with time. When the average size of nanocrystals $\bar{l} = 100$ nm and the experimentally measured diffusion coefficient of the admixture in the particle bulk $q_s = 10^{-20}$ m^2 s^{-1}, this requires a time period of about

$$t_a = \bar{l}^2/q_s = 10^6 \text{ s}. \quad (19)$$

Relation (19) characterizes the duration of the ordering period of the admixture composition of the substance.

The ordering of the admixture composition of the substance can be sketched in the following way. At the nucleation and growth stages, each particle adsorbs any admixture in conformity with the adsorption isotherm

$$\theta_A = B_A C_{admix}/(1 + B_A C_{admix} + B_M C_M),$$

where θ_A is the fraction of the adsorption sites occupied by admixture molecules, C_{admix} and C_M are the admixture and matrix substance concentrations in the medium near the particle, B_A is the adsorption coefficient of the admixture, B_M is the self-adsorption coefficient of the matrix substance.

The two-dimensional clusters formed on the particle surface spread over the surface and thus capture some of the adsorbed admixture; as a result, each section of a new monolayer contains, immediately after deposition, the admixture in the concentration

$$C_{s0} = \chi_A(G)\theta_A.$$

Here, $\chi_A(G)$ is a function characterizing the interaction of the admixture with the spreading cluster. After deposition of this monolayer, the admixture molecules can pass, during the period $\tau = h/G$, into the adsorption layer and then to the medium. Simultaneously, an additional amount of the admixture may pass into the monolayer from the adsorption layer. As a result, within time τ after the monolayer deposition, the admixture concentration in each of its sections can change to reach the value

$$C_{s\tau} = C_{s0}\chi_\tau(G),$$

where $\chi_\tau(G)$ is the function characterizing the admixture redistribution between the monolayer and the medium after the deposition. At time τ, this monolayer section is coated by the next monolayer, *i.e.*, becomes inside the particle bulk. The admixture concentration in the given section changes up to

$$C_s = C_{s\tau}\chi_s(G),$$

where $\chi_s(G)$ is the function that reflects the displacement of the admixture from the given section by the new monolayer.

After the admixture molecules have been coated by the next monolayer, they lose mobility and remain in the particle bulk up to the end of the nucleation and growth stages, so that

$$\frac{dm_A}{dt} = 4\pi \int_0^\infty Gl^2 C_S \varphi(X_i,t)\,dX_i.$$

Here m_A is the amount of the admixture captured by the particles at the nucleation and growth stages.

The functions $\chi_A(G)$, $\chi_\tau(G)$, and $\chi_s(G)$ in the general form are unknown. In some systems, the conditions $B_A C_p \ll 1$, $B_M C_M \ll 1$, $\chi_A(G) = \chi_A = \text{const}$, $\chi_s(G) = 1$, and $\omega_s \neq \omega_s(G)$ hold, so that

$$C_s = [K_E + (\chi_A B_A - K_E)\exp(-\omega_s h/G)]C_{admix},$$

where $K_E = \omega_L/\omega_s$ is the coefficient of the equilibrium distribution of the admixture between the surface monolayer of the given particle and the medium, ω_L and ω_s are the probabilities of transition of an admixture molecule from the medium to the monolayer and back per unit time.

It follows from the foregoing that in an open system where the composition of the medium is maintained invariable, the disorder factor for the admixture composition of the particles is as follows:

$$Z(C_s,t) = [(\chi_A B_A)/K_E]^2 \exp(-2\omega_s h/G). \quad (20)$$

If the growth rate depends slightly on l, then

$$Z(C_s,t) = Z(t). \quad (21)$$

In the case of a closed system, relations (20) and (21) characterize the disorder of the particles at the moment when the concentration of the medium is close to C_{admix} and the rate does not differ much from G.

The foregoing illustrates a common feature of the development of nanosystems, namely, a time lag between ordering and particle enlargement. At the growth stage,

particles compete for the solute and those that grow faster have an advantage. However, the particles that grow faster are more disordered. The ordering of particle composition and structure mainly takes place at the ripening stage when the particles release the admixtures captured out of equilibrium and "heal" the growth defects of the structure.

Complication and degradation of nanosystems

Experiments indicate that during the formation of a nanodispersed substance, the system becomes more complex. The number of nanoparticles in its bulk increases. Both amorphous and crystalline particles appear; moreover, the crystals may be of diverse shapes. Agglomerates are formed and some acquire an hierarchical structure. A variety of impurities and structural defects atypical of equilibrium crystals are accumulated in the nanoparticle bulk. If one takes the number of parameters $\{X_i\}$ that characterize unambiguously the state of the particles as an index of system complexity, one can state that by the end of growth and agglomeration stages, the system becomes most complex. During the ripening and composition ordering, the complexity index decreases if this is not opposed by external impacts on the system.

The decrease in the system complexity is facilitated by the fact that any substance remains in the place where it has been formed only for a limited period of time. Sooner or later it gets into a system whose medium is not saturated enough with respect to the given substance. In man-generated systems, this occurs due to the removal of the substance from the reactor, while in natural ones, this is a result of medium dilution. Immediately after the medium has become unsaturated, vaporization or dissolution of particles starts. The vaporization (dissolution) can proceed at an exceptionally low rate, but this rate is finite. Therefore, if the substance occurs in an unsaturated gas medium, it will completely pass into the vapor after a certain period of time. This time is commensurable with the t_K value determined by the ratio

$$l_M = \frac{\upsilon_0}{\sqrt{2\pi m_0 kT}} \int_0^{t_k} (P_\infty - P)\beta(t)\,dt, \qquad (22)$$

where m_0 is the mass of the molecule, P_∞ is the saturated vapor pressure at the ambient temperature T, P is the partial pressure of the vapor of the given substance at time t, $\beta(t)$ is a function characterizing the retardation of nanoparticle vaporization by adsorbed molecules or by surrounding solids.

The $\beta(t)$ value can be decreased by introducing special additives, which form shielding molecular layers on the nanoparticle surface.[34] The $\beta(t)$ value decreases also upon introduction of nanoparticles into porous solids[35] or application of nanoparticles on substrates, which prevent vaporization.[36] However, $\beta(t) > 0$ in all cases. Therefore, when $P < P_\infty$, the time of existence of any nanoparticles is finite. Since the condition $P < P_\infty$ always holds, it can be concluded that a typical evolution route of a substance obtained from a supersaturated vapor and not subjected to chemical transformations is as follows.

In a vapor whose pressure satisfies condition (11) for $P/P_\infty = C_0/C_\infty$, numerous nanoparticles appear and grow. As a result, the vapor pressure decreases to the level

$$P = P_\infty \exp[l_H/(l_R + l_0)]$$

in time t_1 (Eq. (8)). At time t_1, the vapor starts to leave the system, and, hence, the vapor pressure decreases to a level that randomly varies with time around an invariable average value $\bar{P}$. Due to the decrease in the vapor pressure, the nanoparticles vaporize; complete vaporization of all nanoparticles at $\beta(t) = \beta$, according to relation (22), takes place in time

$$t_K = l_M(2\pi m_0 kT)^{1/2}/[\upsilon_0(P_\infty - \bar{P})\beta].$$

Probably, cyclic routes are also possible; one of them can occur under the following conditions. The saturated vapor with the volume V_0 is compressed to the volume V_1, at which the vapor concentration C corresponds to condition (11), and maintained at $V_1 = \text{const}$ and at a constant temperature during time t_1. Then the system is expanded to the starting volume V_0 and kept at $V_0 = \text{const}$ and the starting temperature during time t_K.

If at $t > t_1$ a reagent capable of entering into a topochemical reaction with nanoparticles gets into the system and the reagent concentration is sufficient for saturation of the medium by the reaction product, the nanoparticles undergo chemical degradation. Each nanoparticle is coated by a layer of the reaction product, which gradually spreads over its bulk. Complete degradation requires time commensurable with t_d.

Principal evolution equation

Numerous experimental data indicate that a one-parameter description of a nanosystem operating by the function $\varphi(l,t)$ is not always adequate. The one-parameter description is based on Eq. (6), which is consistent to a a substantial extent with experimental results in the case of spatially homogeneous systems and an isometric habitus of the nanoparticle.[37,38] However, many real nanosystems are spatially inhomogeneous, being composed of plate-like or filamentous nanocrystals; as a result, for example, in systems containing $Mg(OH)_2$, $Cd(OH)_2$, $EuPO_4 \cdot H_2O$, $BaSO_4$, and $Ca_5(PO_4)_3OH$ nanocrystals, it was necessary to take into account the habitus anisotropy.[39,40] Therefore, it is expedient to pass from a one-parameter to a multiparameter description in which the primary nano-

particles and agglomerates are characterized by eigen functions of state distribution. A change in each of these functions is determined by the equation

$$-\frac{\partial \psi_j}{\partial t} = \mathrm{div}\left(G_{0j}\psi_j - D_{0j}\mathrm{grad}\psi_j\right) + \\ + \sum_{i=1}^{p_j}\frac{\partial}{\partial X_i}\left[G_{ij}\psi - \sum_{K=1}^{p_j}\frac{\partial}{\partial X_K}\left(a_{Kj}G_{Kj}\right)\right] - Q_j, \quad (23)$$

where G_{0j} and D_{0j} are the rate of the directed spatial motion and the diffusion coefficients of particles of sort j, respectively, G_{ij} is the rate of a directed change of one parameter of the inner state of the particles, a_{ij} is the average fluctuation amplitude of the parameter X_i, p_j is the number of parameters describing the state of particles, and Q_j is the intensity of formation of particles of the given sort from particles of other sorts.

Here

$$G_{ij} = (\mathrm{d}x_i/\mathrm{d}t)_j = G(X_i, y_i),$$

$$a_{ij} = a(X_i, y_i), \qquad Q_j = Q(X_i, y_i, \psi_i),$$

and the amplitude a_{ij} of the habitus fluctuations is not substantial enough to violate the condition

$$(a_{ij}/\bar{x}_i) < 0.1,$$

although the scale of fluctuations markedly exceeds the molecular scale.

Equation (23) does not take into account the discrete nature of the addition of molecules to or their abstraction from primary nanoparticles or particles from agglomerates; therefore, it describes only qualitatively the early stages of nucleation. However, the agreement between experimental data and relation (6) indicates that this limitation is insignificant. For many systems, Eq. (23) can be markedly simplified, for example, as applied to later phases of agglomeration or to the ripening. However, this does not deprive this equation of its general meaning.

Conclusion

The experimental data available for nanosystems gives an idea of what phenomena and processes accompany the formation, ordering, and degradation of nanosystems. It is clear that closed systems develop nonmonotonically. During the nucleation, growth, and agglomeration, the morphological and structural diversity is extended, while at the ripening and structural ordering stages, it narrows down. At the initial stage of development, closed nanosystems are disordered, while at the final stage, they are ordered. In open systems, evolution usually leads to disappearance of nanoparticles. In systems of any type, a directed change in the state of particles occurs against the background of substantial fluctuations of process rates, the scale of these fluctuations being much greater than the molecular scale. As a result, the distribution function of particles over state parameters varies according to a Fokker—Planck type equation. This fact may underlie the formulation of the principal equation of the physicochemical evolution of nanosystems based on Eq. (23).

References

1. M. C. Roco, R. S. Williams, and P. Alivisatos, *Nanotechnology Research Directions, I. W. G. N. Workshop Report.*, Kluwer Acad. Publ., Dordrecht, 2000.
2. A. S. Edelstein and R. C. Camarata, *Nanomaterials: Synthesis, Properties and Application*, Inst. Physics. Publ., Bristol—Philadelphia, 1996.
3. I. V. Melikhov and V. E. Bozhevolnov, *J. Nanoparticle Res.*, 2003, **5**, 465.
4. Yu. I. Petrov, *Klastery i malye chastitsy* [*Clusters and Small Particles*], Nauka, Moscow, 1986 (in Russian).
5. I. V. Kazakova, G. V. Godiyak, *Khim. Fizika* [*Chem. Phys.*] 1997, **16**, 118 (in Russian).
6. M. Volmer, *Kinetik der Phasenbildung*, Nh. Steinkopfverb., Dresden—Leipzig, 1939.
7. I. V. Melikhov, E. D. Kozlovskaya, A. M. Kutepov, M. V. Fedotova, V. N. Trosnin, and V. V. Kuznetsov, *Kontsentrirovannye i nasyshchennye rastvory* [*Concentrated and Saturated* Solutions], Nauka, Moscow, 2002 (in Russian).
8. V. F. Komarov, A. V. Severin, and I. V. Melikhov, *Crystalografiya*, 2000, **45**, 364 [*Crystallogr. Repts*, 2000, **45** (Engl. Transl.)].
9. I. V. Melikhov, V. F. Komarov, and Yu. A. Kozel, *Kolloid. zh.*, 1988, **49**, 690 [*Colloid. J. USSR*, 1988, **49** (Engl. Transl.)].
10. D. Balarev, *Stroezh na realnokristalnite sistemy*, Nauka i izkustvo, Sofia, 1964.
11. N. P. Yushkin, *Teoriya microblochnogo rosta crystalov v prirodnykh geterogennykh rastvorakh* [*Theory of Microblock Crystal Growth in Natural Heterogeneous Solutions*], Komi FAN SSSR, Syktyvkar, 1971 (in Russian).
12. I. V. Melikhov and V. G. Pechnikov, *Zh. Fiz. Khimii*, 1970, **44**, 2239 [*Russ. J. Phys. Chem.*, 1970, **44** (Engl. Transl.)].
13. I. V. Melikhov, E. N. Kitova, A. N. Kamenskaya, N. B. Mikheev, and S. A. Kulyukhin, *Kolloid. Zh.*, 1997, **59**, 78 [*Colloid. J.*, 1997, **59** (Engl. Transl.)].
14. N. B. Mikheev, I. V. Melikhov, and A. N. Kamenskaya, *Radiokhimiya*, 1997, **39**, 523 [*Russ. Radiochem.*, 1997, **39** (Engl. Transl.)].
15. I. V. Melikhov, S. B. Baronov, and S. S. Berdonosov, *Zhurn. Fiz. Khimii*, 2004, **78**, 1794 [*Russ. J. Phys. Chem.*, 2004, **78** (Engl. Transl.)].
16. I. V. Melikhov, E. D. Kozlovskaya, L. B. Berliner, and M. A. Prokofiev, *J. Colloid. Interface Sci.*, 1987, **117**, 1.
17. I. V. Melikhov, *Zh. Fiz. Khimii*, 1989, **63**, 476 [*Russ. J. Phys. Chem.*, 1989, **63** (Engl. Transl.)].
18. L. B. Berliner and I. V. Melikhov, *Teoret. Osnovy Khim. Tekhnologii*, 1985, **19**, 24 [*Theor. Foundations Chem. Technol.*, 1985, **19** (Engl. Transl.)].

19. I. V. Melikhov and B. D. Nebylitsin, *Rost crystallov* [Crystal *Growth*], Izd. Erevanskogo Univ., 1977, **12**, 103 (*in Russian*).
20. O. M. Todes, V. A. Seballo, and A. D. Gol´tsiker, *Massovaya Crystalizatsiya iz Rastvorov*, Khimiya, Leningrad, 1984 (in Russian).
21. P. H. Singer, *Semiconductor International*, 1998, **21**, 111.
22. I. V. Melikhov and G. Vucovic, *Radiochim. Acta*, 1998, **77**, 83.
23. I. V. Melikhov, V. A. Prisyazhnyuk, *Crystalografiya*, 1978, **23**, 595 [*Sov. Phys.-Crystallogr.*, 1978, **23** (Engl. Transl.)].
24. V. E. Bozhevolnov, L. N. Ivanov, V. K. Kozlov, V. V. Voronov, Yu. P. Timofeev, and V. V. Karelin, *Phys. Stat. Sol.*, 1976, **78**, 483.
25. V. V. Karelin, Yu. N. Orlov, V. E. Bozhevol´nov, L. N. Ivanov, *Vestn. MGU*, *Seriya 2. Khimiya*, 1981, **22**, 63 [*Vestn. Mosk. Univ., Ser. Khim.*, 1981 (Engl. Transl.)].
26. V. I. Aleshin, V. E. Bozhevol´nov, L. N. Ivanov, V. V. Karelin, *Izv. Akad. Nauk SSSR*, *Ser. fiz.*, 1986, **50**, 571 [*Bull. Acad. Sci. USSR, Div. Phys. Sci.*, 1986 (Engl. Transl.)].
27. I. V. Melikhov, V. M. Podkopov, B. A. Ilyin, and E. D. Kozlovskaya, *Chem. Eng. Sci.*, 1996, **51**, 671.
28. R. Kaischev and E. Budevski, *Contemp. Phys.*, 1967, **8**, 489.
29. J. D. Wright and N. A. J. M. Sommerdijk, *Sol-Gel Materials: Chemystry and Applications*, Taylor and Francis, New York, 2001.
30. E. I. Suvorova, L. E. Popak, V. F. Komarov, and I. V. Melikhov, *Crystalografiya*, 2000, **45**, 1520 [*Crystallogr. Repts*, 2000, **45** (Engl. Transl.)].
31. I. V. Melikhov, E. N. Kitova, A. Ya. Gorbachevskii, Yu. D. Perfil´ev, V. P. Shantarovich, I. O. Bogatyrev, I. B. Kevdina, and A. L. Nikolaev, *Zh. Fiz. Khim.*, 1993, **67**, 75 [*Russ. J. Phys. Chem.*, 1993, **67** (Engl. Transl.)].
32. I. V. Melikhov, Zh. Vukovich, B. D. Nebylitsin, *Zh. Fiz. Khim.*, 1972, **46**, 1952 [*Russ. J. Phys. Chem.*, 1972, **46** (Engl. Transl.)].
33. I. V. Melikhov and M. S. Merkulova, *Socrystalizatsiya* [*Co-Crystallization*], Nauka, Moscow, 1975 (in Russian).
34. P. M. Ajayan, L. S. Schlager, and P. V. Braun, *Nano-composite Science and Technology*, Willey-VCH Verlag, Weinheim, 2003.
35. S. Mann, *Biomineralization: Principle and Concepts in Bioinorganic Materials Chemistry*, Oxford Univ. Press., Oxford, 2002.
36. G. M. Whitesides, J. P. Mathias, and C. T. Seto, *Science*, 1991, **254**, 1312.
37. I. V. Melikhov and A. S. Kelebeev, *Crystalografiya*, 1979, **24**, 410 [*Sov. Phys.-Crystallogr.*, 1979, **24** (Engl. Transl.)].
38. I. V. Melikhov, A. S. Kelebeev, and S. Bacic, *J. Colloid Interface Sci.*, 1986, **53**, 784.
39. I. V. Melikhov, M. Ya. Belousova, N. A. Rudnev, N. T. Buludov, *Crystalografiya*, 1974, **19**, 784 [*Sov. Phys.-Crystallogr.*, 1974, **19** (Engl. Transl.)].
40. V. F. Komarov, A. G. Chaliyan, I. V. Melikhov, *Zh. Neorg. Khim.*, 1966, **41**, 533 [*J. Inorg. Chem. USSR*, 1966, **41** (Engl. Transl.)].

Received December 1, 2004;
in revised form December 27, 2004